ALTERATION OF GRANITE AND MONZONITE FROM THE NORTHERN BLACK FOREST, GERMANY

– EVIDENCE FROM HYDROTHERMAL EXPERIMENTS AT 70°C AND 200°C

Ingrid Stober [1], Kirsten Drüppel [1], Jens C. Grimmer [1] and Paula Niemitz [1]

[1]Karlsruhe Institute of Technology, Institute of Applied Geosciences, Adenauerring 20b, D-76131 Karlsruhe, Germany

Ingrid.stober@kit.edu

Keywords: *Alteration-experiments, granite, deep circulating fluids, water-rock-interaction, hydrochemistry.*

ABSTRACT

In order to better understand their alteration processes, granites and monzonites from the northern Black Forest have been reacted as rock powder with bi-distilled water at temperatures of 70°C and additionally as cylindrical rock samples with a 2-molal NaCl-H_2O solution at 200 °C in autoclaves for 36 days. Rock powder after the 70°C experiments was not investigated but the resulting leaching fluids of the low temperature experiments showed enhanced concentrations of K, Na, Ca and other parameters, with higher TDS being recorded by the monzonites. Thus, even by low temperature experiments alteration reactions could be observed. The main minerals affected by dissolution during the high temperature experiments are plagioclase and K-feldspar, quartz, biotite and chlorite, irrespective of the rock type. In the marginal zones of the rock samples, K-feldpar is partly replaced by albite, whereas biotite reacted to chlorite and hematite. Precipitates on the sample surfaces include illite, hematite, and analcime. The solutions after the high temperature experiments showed enhanced concentrations of K, Ca, Si and other parameters, not present at the beginning of the experiments and are thus originating from alteration and partial dissolution of plagioclase, K-feldspar, quartz, biotite, and chlorite. The solutions were partially saturated, partially undersaturated with respect to quartz. Certain elements (e.g., Na, Fe, Al) were subsequently incorporated into the solids precipitated during the experiments or adsorbed onto mineral surfaces and cannot be considered as conservative. The alteration process is simulated by using stability diagrams.

1. INTRODUCTION

Deeply buried Variscan crystalline basement rocks contain and conduct water in several km depths. Na-Cl brines of about 100 g/kg TDS are the prevailing fluids (Pauwels et al. 1993, Stober & Bucher 2015). Interaction of these circulating fluids with the respective reservoir rock may drastically alter the composition of both fluid and host rock. The study focuses on fluid-rock-interaction processes (i.e. mainly dissolution and precipitation) of intact sawed granites and monzonites samples of the Black Forest (as proxy for fracture surfaces) under reservoir conditions, i.e. with NaCl-rich thermal waters at 200°C temperature. Additionally, we simulated the recharge conditions into these deep reservoirs by carrying out leaching experiments with rock powder in pure water at temperatures of 70°C.

Dissolution and precipitation processes influence permeability at the micro- to reservoir scale. Our approach allows investigating experimentally the conditions under which a solid or fluid phase forms or changes as a function of the composition of the surrounding fluid at given temperatures. In this experimental study, we simulate the alteration, e.g. the reaction of different types of granites and monzonites in contact with i) bi- distilled water at 70˚C and ii) a synthetic 2 molal Na-Cl solution at 200°C to understand in detail early stage WRI-processes taking place i) during recharge, e.g. along the descending path (infiltration of meteoric water, Fig. 1), and ii) within the deep reservoir.

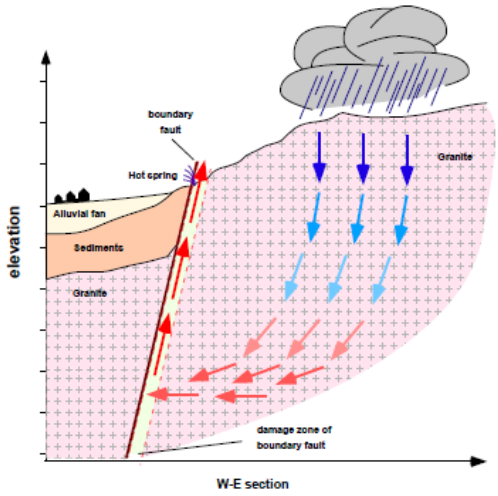

Figure 1: Fault zones, ascend paths for thermal waters from deep reservoirs (after Stober et al. 2016)

2. GEOLOGY AND HYDROGEOLOGY OF THE STUDY AREA

The crystalline basement of the Black Forest is exposed in southwestern Germany as a c. 130 km long and 40 km wide N-S trending erosional window through the cover sediments. Except for the northernmost Baden–Baden Zone, it belongs to the Moldanubian zone of the Variscan belt. The crystalline basement consists predominantly of high-grade para- and orthogneisses, partly magmatic, intruded by a number of post-collisional carboniferous granites (e.g. Emmermann, 1977). To the east the basement rocks are overlain by Permotriassic to Jurassic sedimentary rocks, whereas they are bounded by the Upper Rhine Graben to the west (Fig. 2).

Our study comprises 30 granite and granodiorite and 15 monzonite samples from various localities in the Black Forest (Fig. 2).

The c. 500-1500 m high eastern graben shoulder of the Schwarzwald exposes Variscan Carboniferous granites and gneisses and post-Variscan Permian rhyolitic rocks (Fig. 2).

Surface exposure and topography are important boundary conditions for i) the entrance of meteoric fluids into crystalline basement rocks and ii) for the formation of a hydraulic gradient that can drive fluids along a deep circulation path and into deeper parts of the crystalline basement rocks (Fig. 1). The high hydraulic gradient of ~0.2 (topographically induced) is the ‚motor' for infiltration in deeper parts of the crust (descending part of the circulation) and ascending along zones of higher permeability (e.g. Grasby & Hutcheon 2001, Stober & Bucher 2015). Thus depth of circulation depends on the hydraulic gradient. Typically, the deep fluids are upwelling along high permeable, steep structures, e.g. within the so called damage zones of faults within the crystalline basement, as for example thermal springs in crystalline basement rocks, like Baden-Baden, etc. These high permeable structures are necessary to drain, collect and transport deep thermal waters to the surface. As cataclastic faults commonly develop less permeable, clay-rich gouge in the fault core during progressive deformation, fault cores may act as a hydraulic barrier forcing deep thermal water to ascend (Fig. 1). Thus, fault zones may often be associated with both very low (fault core) and enhanced permeability (damage zone) (e.g. Choi et al. 2016).

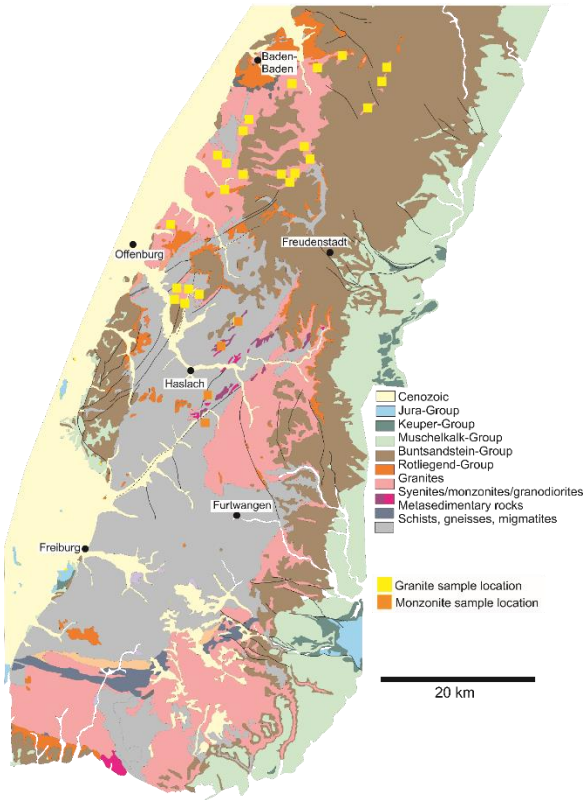

Figure 2: Geological map of the Schwarzwald crystalline basement in SW Germany, showing sampling sites.

Infiltration of cold, low mineralized meteoric water (precipitation) is relatively slow due to the low to moderate natural permeability of the crystalline basement rocks (Fig. 1). The mineralization of the descending water (meteoric origin) will increase due to alteration of the granitic rocks (water rock interaction, WRI) and water gets a 'granitic signature'. Reactions between descending water and the fractured rock, e.g. the minerals, gradually change with increasing pressure and temperature (p, T). At reservoir depth, residence time and high temperature is high enough for establishing partial equilibration (e.g. Stober & Bucher 1999).

In contrast to the very slow descent, ascent of deep thermal water along the permeable damage (or fracture) zone must be rather fast, to induce a spring with enhanced temperature (López & Smith 1995, Stober et al. 2016). During upwelling changing p/T-conditions cause some minerals to precipitate and hence to clog flow-paths, leading to a reduction of permeability. Thus, continuously flowing thermal springs require tectonically active areas (earthquakes), re-activating the flow path, as a continuous process.

3. METHODS

3.1 Experimental setup

Leaching experiments were carried out at 70°C in glass batch reactors at a constant temperature of 70 °C with 20 g of rock powder (grain size <40 µm) in 160 ml bi-distilled water. Fig. 2 shows the localities of the different rock samples in the northern Schwarzwald, used for the leaching experiments. During the experiments the liquid was constantly mixed by an external magnetic stirrer (500 rpm), and electrical conductivity as well as pH were continuously measured. When constant values (el. cond., pH) were achieved, leaching experiments were stopped. During the leaching experiments the glass batch reactors were closed, to prevent evaporation. The leaching fluid was centrifuged and filtrated (0.45 µm). For cation analyses, water samples were acidified (65% HNO_3), for anion analyses not. All samples were stored in 30 ml polyethylene bottles and preserved cool until analysis. Major and minor cations were measured by inductively-coupled plasma mass spectrometry (ICP-MS) using a Thermo Fischer Scientific X-Series and anions by a Dionex ICS 1000. Carbonate was measured by titration and bromide by using a Dionex ICS 2100. Dissolved SiO_2 concentrations were analyzed partly photometrically and partly by inductively-coupled plasma optical emission spectrometry (ICP-OES) with a Varian 715 ES. The latter method produced unrealistic high values related to dissolved SiO_2. Thus, for further investigations we neglected these results.

Batch-type alteration experiments at 200°C were performed in hydrothermal autoclaves (stainless steel vessels with teflon inlets). Each autoclave has total volume of 90 ml. In contrast to the leaching experiments, in which we used rock powder, the alteration experiments were carried out with cylindrical granitic rock samples. A 2-molal NaCl solution (116.9 g/kg) was prepared, mixing deionized water and NaCl, in accordance with the main brine components found in the deep subsurface (TDS of 94-200 g/l, Stober & Bucher, 2014). The 2-molal Na-Cl solution already depicts the natural reservoir fluid composition chemically by 88–94 mol.% (Pauwels et al. 1993). Small amounts of inorganic carbon (alkalinity of <0.1mmol l^{-1}) and O_2 are dissolved in the initial solution due to contact with the atmosphere. The initial pH of the solution was 5.5, measured at 25 °C. A total of 19 cylindrical rock samples (14 granites, 5 monzonites), collected in outcrops in the northern Schwarzwald (Fig. 2), were prepared, 5-15 mm long and 15-25 mm in diameter. Samples were washed with de-ionized water and dried before the experiment. Together with the 2-molal NaCl-solution, the rock cylinders were stored in the autoclaves and heated at 200°C for 36 days. Pressures during experiment are about 16 bar, given by the boiling conditions of the Na-Cl solution.

3.2 Analysis of the fluid

Analysis of fluids of the experiments at 70°C is already described in section 3.1.

Fluids of the experiments at 200°C were cooled down rapidly after each experiment to room temperatures. Electric conductivity (Mettler Toledo Inlab 371) and pH (ProMinent PHER-112) were measured immediately. Carbonate alkalinity was determined by titration with 0.01 M HCl. The experiment solution was filtered with a 0.45 µm cellulose acetate membrane for further fluid analyses. To ensure solution stability, the fluid samples were diluted with ultra-pure water by a factor of 10 and, for cation measurements, acidified with distilled HNO_3. Samples were stored in 30 ml polyethylene bottles and preserved cool until analysis.

Major and minor elements were determined by inductively-coupled plasma mass spectrometry (ICP-MS) with a Thermo Fischer Scientific X-Series 2. Sample dilution was 1:100. Dissolved Si and Na concentrations were analyzed by inductively-coupled plasma optical emission spectrometry (ICP-OES) with a Varian 715 ES instrument and a sample dilution of 1:200 for Si and 1:500 for Na. Ion chromatography (IC) was performed with a Dionex, ICS-1000 instrument for dissolved anions. Due to high concentrations of Cl and a consequential need for high dilution of the sample (1:2000), it was not possible to detect other anions than Cl. Quality of fluid measurements was verified by continuous measurement of standard solutions during analysis procedure. Accuracy of ICP-MS measurements is better than 3% for main cations and better than 8% for Al and Fe, for ICP-OES better than 5% and for IC better than 4%.

3.3 Analysis of the solids

The initial chemical rock composition of all granite and monzonite samples was analyzed by X-ray fluorescence (XRF) and ICP-MS. For the analysis, rock samples were crushed and grinded to powder. Analyses of the main elements were performed on prepared fusion beads with a wave length dispersive Bruker S4Pioneer instrument.

The trace element geochemistry of the rock samples before the experiment was determined by ICP-MS with a Thermo Fisher X-series 2 instrument after HNO_3-HF-$HClO_4$ acid digestions of the powdered material (100 mg). To assure a complete silicate decomposition, 40% HF (suprapur), 70% $HClO_4$ (normapur) and the pre-oxidized sample (65% HNO_3, sub-boiled) was heated in a closed vessel for 16 h at 120 °C. After evaporating the acids to incipient dryness, the residue was re-dissolved in 65% HNO_3 and evaporated again (three times) for purification purposes. The final residue was dissolved in 50 mL of ultrapure water. To assure the quality of the whole procedure, three blanks and two certified reference materials (GS-N, SY-2; Govindaraju 1994) were included into the digestion process (accuracy: ±10%). The reproducibility (±5% for most elements) was checked by digesting one sample in triplicate. The quality assurance for the ICP-MS measurement was done by including the certified reference material CRM-TMDW-A (High-Purity standards, Inc.) into the protocol (accuracy: ±7% for most elements).

Reacted rock samples of the experiments at 200°C were removed from the vessel after solution extraction and washed with deionized water to avoid halite precipitation. However, some samples showed nevertheless halite crystals on the rock surface. Afterwards, the samples were dried at room temperature. Characterization of the initial and post-experiment rock samples (both the original and reacted rock surfaces and corresponding thin sections) was performed with different analytical and imaging methods.

Alteration processes on sample surfaces and cross-sectional thin sections were analyzed by environmental scanning electron microscopy (SEM) with a Philips ESEM XL 30. Surface investigation was performed mainly in secondary electron (SE) mode with an acceleration voltage of 10 kV. Additionally, thin sections were examined for alteration reaction textures in the sample interior under back-scattered electron (BSE) mode at the same setting. Mineral identification and qualitative analyses have been conducted with energy-dispersive X-ray spectroscopy (EDX) of the SEM.

Electron microprobe (EMP) measurements were carried out with a JEOL JXA-8530F. Calibration was performed on the following natural standards: Al: Al_2O_3, Ca and Si: wollastonite, Fe: Fe_2O_3, Mn and Ti: $MnTiO_3$, K: orthoclase, Na: albite, Mg: MgO, F: CaF_2, and Cl: NaCl. Measuring conditions were an acceleration voltage of 15 kV, a beam current of 20 nA and a beam diameter of 1 mm for all mineral phases except analcime (beam size of 2-4 mm depending on grain size). Detection limit was 0.01 wt%.

4. RESULTS

4.1 Composition of the starting material

Petrographical investigations of the granites of the Northern Schwarzwald concentrated on 47 samples. These samples mainly comprise medium grained biotite granites and two-mica granites. Rare muscovite granites and tourmaline granites are exposed locally. The mineral modes of the granites are variable, with increasing amounts of biotite (X_{Mg}: 0.30-0.42) and plagioclase (An_{0-30}) being accompanied by decreasing amounts of quartz, K-feldspar, and white mica. Minor amounts of ilmenite and hematite are present in all samples, but most prominent in the biotite granites.

The 13 samples of the comparably rare, medium grained monzonites show equigranular to weakly porphyritic textures and are mainly composed of plagioclase (An_{21-36}), biotite (X_{Mg}: 0.28-0.39), and – in part of the samples – amphibole. K-feldspar and quartz are present in some of the samples as minor phases.

Mineral chemistry: Plagioclase displays normal concentric zoning with a rimward decrease of its anorthite contents. The values range from 21-36 mol% (oligoclase and andesine) in monzonites to 0-30 mol% (albite and oligoclase) in granites. Anorthite contents increase with increasing amounts of biotite and plagioclase and decreasing Si. K-feldspar is micro- to mesoperthitic potassium feldspar (microcline and occasional orthoclase), with a potassium feldspar host (Or_{89-100}), bearing albite (Ab_{97-99}) exsolution lamellae. The An-contents of K-feldspar reach up to 0.9 mol.%. Biotite of the granites and monzonites show a similar Fe-rich composition with the X_{Mg}: values ranging between 0.30-0.42 in the granites and 0.28-0.39 in the monzonites. Igneous white mica of the two mica and muscovite granites is the almost pure muscovite endmember with slightly increased Ti, Fe, and Mg contents. Extreme enrichment of a second generation of white mica of a similar composition, coexisting with chlorite, is observed in part of samples which also underwent

deformation. Greenish chlorite (X_{Mg}: 0.28-0.38) replaces biotite. The chlorites display significant differences in their X_{Mg}, depending on composition of the precursor biotite. Ilmenite, rutile, and hematite are the main Fe-(Ti) oxides present. The MnO contents of ilmenite range between 2 and 9 wt.%. Hematite intergrown with chlorite, is the almost pure endmember. Rutile attains Nb values of up to 1 wt.%. Carbonate replacing plagioclase is virtually pure calcite. Apatite is fluorapatite with high F-contents of 5-7 wt.%.

Geochemical analyses of granites and the monzonites are illustrated in Fig. 3. The SiO_2 contents of the granites range between 70 wt.% and 78 wt.%, whereas those of the monzonites are distinctly lower (55–67 wt.%). As shown in the $Na_2O+ K_2O$ versus SiO_2 classification diagram of Middlemost (1994), granites plot in the granite field. The samples designated as monzonite on the basis of the petrographic investigation have a much more variable composition, mainly ranging from monzonite to quartz-monzonite, but subordinately also comprising diorite, and syenite (Fig. 3). For clarity they are grouped together as `monzonites´.

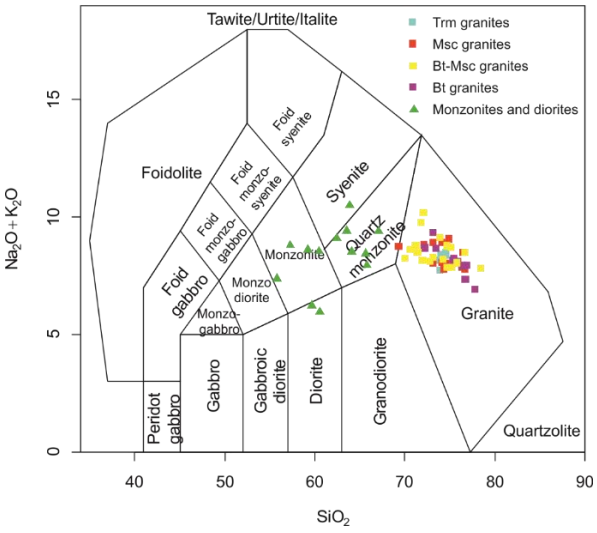

Figure 3: Classification diagram (Middlemost 1994) for granites and monzonites of the northern Schwarzwald.

4.2 Composition of the fluids in the leaching and alteration experiments

Leaching experiments (70°C): Despite the low temperatures, the composition of the fluids strongly changed during the experiments. The pH values of leachates range between 6.0 and 8.8, whereas most values group between 7.0 and 8.0. Highest pH values are obtained for the leachates of the monzonites (median: pH = 8.1) and lowest for muscovite- and muscovite-biotite-granites (median: 7.35). Total dissolved solids (TDS) are presented in this context without SiO_2-concentration, since SiO_2 was measured with two different methods leading to very different results. Thus, TDS* (-SiO_2) vary between 37 mg/l and 204 mg/l. Generally, leachates of the monzonites show the highest TDS* with a median value of 102 mg/l. Relatively low TDS* were measured in the fluids of the muscovite- and biotite-granite experiments (median: 66 mg/l and 58 mg/l).

In most experiments potassium was the dominant cation, followed by sodium, reaching concentrations of up to 30 mg/l, resp. 25 mg/l. However, in few experiments sodium was the main cation. The highest Na-concentrations were measured in the Bt-Ms- and Ms-Bt-granite leachates (median: 14 mg/l and 11 mg/l), while the highest K-concentrations were achieved in the leaching experiments with monzonite (median: 20 mg/l). Calcium and magnesium generally showed very low concentrations. In only few experiments calcium reached concentrations of more than 5.0 mg/l. The median of the Ca-concentration in all experiments was below 0.7 mg/l. In contrast, the Mg-concentration in the monzonite leachates was significantly higher (median: 1.1 mg/l) than in all other experiments. Chloride-concentration was with a median value of 12 mg/l surprisingly high. Some samples even showed concentrations of more than 30 mg/l. The highest median values were achieved in the experiments with Bt-Ms- and Ms-Bt-granite (14.7 mg/l and 14.1 mg/l). The experiments with monzonite showed the highest SO_4- and HCO_3-concentrations (median: 2.6 mg/l and 60 mg/l). Bromide was detectable in all samples (between 0.20 and 1.15 mg/l) The leaching experiments with monzonite showed higher Fe-, Ba-, and Li-concentrations in comparison to the other experiments.

Alteration experiments (200°C): The pH values of fluids after experiment range between 4.6 and 8.8 (measured at room temperature), whereas the alteration experiments with granites showed generally lower pH (about 5.0) than the experiments with monzonites (> 6.0). Sodium concentrations are generally high, due to the originally NaCl-rich composition of the synthetic fluid. Thus, our further investigations focus on the new components in the fluid due to WRI.

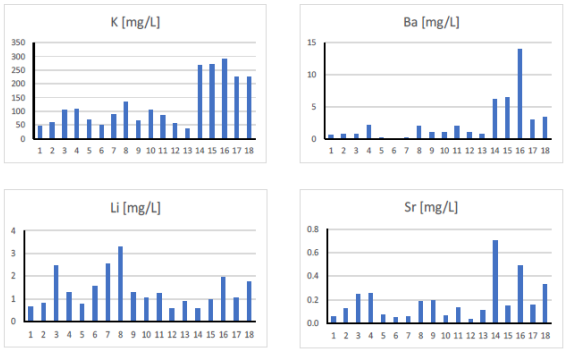

Figure 4: Selected fluid parameters of the alteration experiment. No 1-2: Ms-granite, 3-7: Ms-Bt-granite, 8-13: Bt-granite, 14-18: monzonite.

Concentrations of most cations increased with respect to the values of the initial solution, with monzonites showing higher cation concentrations (252 – 402 mg/l) than granites (61 - 202 mg/l). Potassium concentrations are comparably high in the fluids of all experiments, whereas Ca and Mg are generally low. The higher cation concentrations in the monzonite-fluids are mainly caused by higher potassium values in these fluids (225 - 290 mg/l) in comparison to the granites (35 – 135 mg/l). Ba is as well increased in the fluids that resulted from interaction with monzonite. Elevated concentrations of Sr and Tl are predominantly observed in monzonite-fluids too, whereas some fluids of the granite experiments showed enhanced Li values (Fig. 4). SiO_2 concentrations in the fluids are relatively high, between 40 mg/l and 107 mg/l, but the fluid is still undersaturated with

respect to quartz. We could not observe any difference between monzonite and granite.

4.3 Reaction textures of rock samples after the hydrothermal experiments (200°C)

After experiments, etch pits are found on the exposed mineral surfaces in all reacted samples, mainly concentrating along grain boundaries and on the crystal surfaces of the feldspars and quartz and subordinately of biotite. Quartz shows numerous, sub-rounded pores of up to 2 µm in diameter and smoothening of fracture edges (Fig. 5a). It forms morphological rises on most sample surfaces.

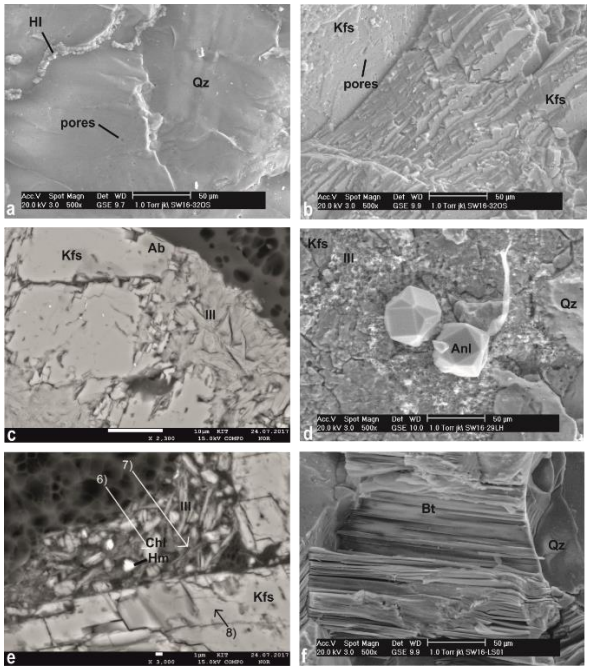

Figure 5: SEM pictures of reaction textures in granites and monzonites after hydrothermal experiments at 200°C. (a, b, d, e): SE pictures; (c, f): BSE pictures. (a) Quarz shows small pores and smoothening of the fracture edges. (b) Elongated dissolution pits in K-feldspar. (c) Both albite and illite replace K-feldspar during experiment. (d) Euhedral analcime, grown on K-feldspar. (e) Chlorite-hematite-illite intergrowth on K-feldspar. (d) Open cleavage of biotite.

Both K-feldspar and plagioclase show minor smoothening of grain edges and cleavages. Deep and elongated dissolution pits are oriented parallel to the well-developed cleavage (Fig. 5b). In marginal zones of the cross-sectional thin sections, narrow irregular reaction fronts can be observed along the K-feldspar grain boundaries, where K-feldspar is replaced by albite (Fig. 5c). Both K-feldspar and the secondary albite are surrounded by accumulations of tiny illite flakes. Moreover, illite precipitates were found on the mineral surfaces of plagioclase and quartz but show a clear preference of K-feldspar (Fig. 5d). Locally, illite is associated with tiny hematite microcrystallites and/or chlorite (Fig. 5e). In three of the 19 samples (preferentially monzonites), both illite and hematite are overgrown by euhedral analcime crystals of 30-50 µm in diameter (Fig. 5d). Biotite is characterized by an expansion of its cleavage planes, possibly caused by its partial replacement by chlorite (Fig. 5f). Newly formed chlorite at the sample margins exposes a brownish color, due to its intergrowth with dust-like hematite or rutile.

5 DISCUSSION

5.1 Leaching experiments

In the leaching experiments we observed as dominant cations potassium and sodium. Generally, possible simplified reaction-equations of water-rock interaction (WRI) with the different granites are the dissolution of K-feldspar and plagioclase (with an albite- and anorthite-component), leading to an enrichment in K and Na in solution, forming kaolinite as alteration-product and additionally to an increase of HCO_3 in solution (Bucher & Stober 2002) (Fig. 14, eq. 1, 2, 3).

K-feldspar:

$$4KAlSi_3O_8 + 6H_2O + 4CO_2 \longrightarrow 2Al_2Si_2O_5(OH)_4 + 8SiO_{2eq} + 4K^+ + 4HCO_3^- \quad (1)$$

albite:

$$4NaAlSi_3O_8 + 6H_2O + 4CO_2 \longrightarrow 2Al_2Si_2O_3(OH)_4 + 8SiO_{2eq} + 4Na^+ + 4HCO_3^- \quad (2)$$

anorthite:

$$CaAl_2Si_2O_8 + 3H_2O + 2CO_2 \longrightarrow Al_2Si_2O_5(OH)_4 + Ca^{2+} + 2HCO_3^- \quad (3)$$

According to the geochemical investigations the anorthite-component of plagioclase in the investigated granites is - in contrast to the monzonites - relatively low and the corresponding albite-component relatively high. However, according to Lasaga et al. (1994) and Froger & Schweda (1998), higher dissolution rates are expected from anorthite than from albite or K-feldspar. Thus, in the following all three alteration processes are discussed (eq. 1, 2, 3).

During the leaching experiments in closed glass batch reactors the atmospheric CO_2 is a limiting factor, thus H^+ will be consumed progressively, leading to an increase of pH in the solution (eq. 4), as measured in the experiments.

$$2KAlSi_3O_8 + H_2O + 2H^+ \longrightarrow Al_2Si_2O_3(OH)_4 + 4SiO_{2eq} + 2K^+ \quad (4a)$$

$$2NaAlSi_3O_8 + H_2O + 2H^+ \longrightarrow Al_2Si_2O_3(OH)_4 + 4SiO_{2eq} + 2Na^+ \quad (4b)$$

$$CaAl_2Si_2O_8 + H_2O + 2H^+ \longrightarrow Al_2Si_2O_5(OH)_4 + Ca^{2+} \quad (4c)$$

Looking into detail, with progressive alteration of albite the concentration of sodium and SiO_2 in the fluid will increase, thus on the surface of albite Na-beidellite (expressed as $NaAl_7Si_{11}O_{36}H_6$) will develop surrounded by kaolinite (eq. 5), whereas progressive alteration of K-feldspar leads to an increase in potassium in solution and illite (expressed in eq. 6 as muscovite, $KAl_3Si_3O_{10}(OH)_2$), followed by kaolinite will form (eq. 6). Please note the reaction described with eq. 6 is in contrast to eq. 5 independent on $SiO_{2(aq)}$.

$$2NaAl_7Si_{11}O_{36}H_6 + 2H^+ + 7H_2O = 7Al_2Si_2O_5(OH)_4 + 2Na^+ + 8SiO_2 \quad (5)$$

$$2KAl_3Si_3O_{10}(OH)_2 + 2H^+ + 3H_2O = 3Al_2Si_2O_5(OH)_4 + 2K^+ \quad (6)$$

Activity diagrams were prepared (Fig. 6, 7). The water compositions of the 70°C-leaching experiments were recalculated in terms of component activities by using the code PHREEQE (Parkhurst et al. 1980).

The sodium-potassium ratio is one of the most fundamental relationships in the waters of the 70°C-leaching experiments, since the main components in the solution are K and Na. The Na-K stability diagram (Fig. 6) shows the dependency of the Na- and K-activity on pH (expressed as H^+) at 70°C and for two different saturation states with respect to quartz (SI_{Qz} = 0.0, SI_{Qz} = -0.15). Since the photometrically determined SiO_2-concentrations, showing lower concentrations, are more realistic, we assume undersaturation with respect to quartz (red phase boundaries in Fig. 6). The presented activity diagram is calculated for illite, a K-sheetsilicate with 50% geochemical pure muscovite (endmember).

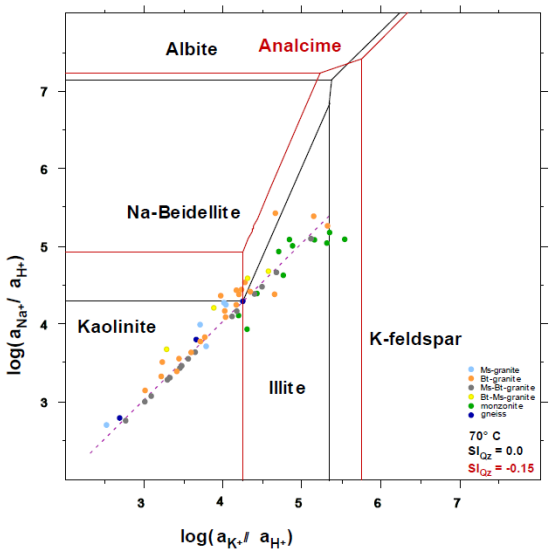

Figure 6: Stability diagram of K vs. Na activity of the leached waters in dependence of pH for 70°C, atm. pressure and different quartz saturation states, calculated with the thermodynamic program MacIIPtax (Brown et al., 1989) on the basis of thermodynamic data of Helgeson et al. (1981), Berman (1988), Liou et al. (1991) and phase plotter of Lieberman (1991).

Fig. 6 shows that the phase boundary between kaolinite and illite is independent of SI_{Qz} (eq. 6), in contrast to the phase boundary between kaolinite and Na-beidellite, shifting in vertical direction with decreasing SI_{Qz} (see eq. 5). Due to undersaturation with respect to quartz a new stability field for analcime develops. The leached water samples plot into the kaolinite- and illite-window and can be fitted to one continuous line with a slope of m = 1 (violet line in Fig. 6). Thus, the fluids will develop along this line, a parallel to the metastable extension of the albite (resp. analcime) – K-feldspar phase boundary, until saturation with respect to K-feldspar is achieved. They will then evolve along this vertical phase boundary until saturation with respect to albite, resp. analcime, is reached, depending on the saturation state with respect to quartz. Fig. 6 shows that the monzonites are the most reactive rocks used in our experiments. Thus, the monzonite-fluids are the most evolved fluids, plotting more or less exclusively in the illite-window. Whereas the leaching experiments with muscovite-granite show significantly lower reactions: all samples plot in the kaolinite-window. On the other hand, muscovite-biotite-granites show significantly lower reactivity then biotite-muscovite- or biotite-granites.

Similar phase diagrams were calculated for Ca- and Na-activity in dependence of pH (expressed as H^+) at 70°C and for two different saturation stats with respect to quartz (SI_{Qz} = 0.0, SI_{Qz} = -0.15). With decreasing SI_{Qz} the kaolinite-window is increasing (Fig. 7). Fig. 7 shows calcite saturation at atmospheric CO_2 pressure. With decreasing CO_2-pressure, i.e. during the leaching experiments in closed glass batch reactors, calcite saturation will be reached by higher log (a_{Ca2+}/a^2_{H+})-values, implying undersaturation of the leached waters with respect to calcite. This observation is in agreement with the calculation of saturation indices using the code PHREEQE (Parkhurst et al. 1980).

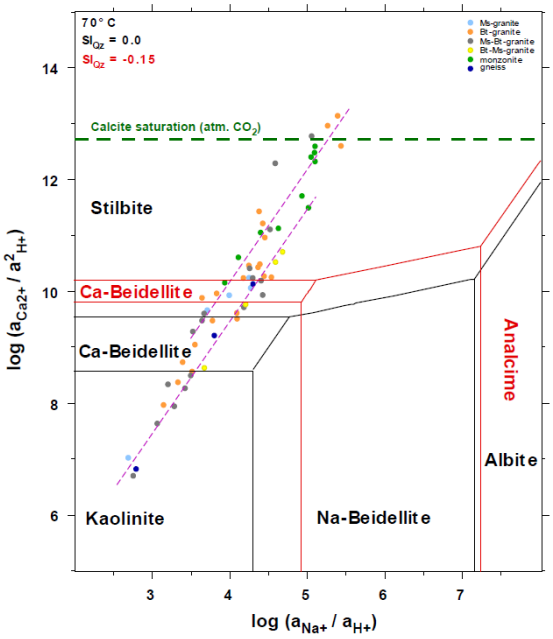

Figure 7: Stability diagram of Na vs. Ca activity of the leached waters in dependence of pH for 70°C, atm. pressure and different quartz saturation states, calculated with the thermodynamic program MacIIPtax (Brown et al., 1989) on the basis of thermodynamic data of Helgeson et al. (1981), Berman (1988), Liou et al. (1991) and phase plotter of Lieberman (1991).

All water samples of the leaching experiments plot into the kaolinite-, the Ca-beidellite- and the stilbite-field, i.e. the fluid in contact with plagioclase will produce clay-minerals and zeolites. Fig. 7 shows that the monzonite- and some Ms-granite-fluids are the most evolved fluids. The monzonite-fluids plot more or less exclusively in the stilbite (a Ca-zeolite) field. The data can be fitted to two continuous lines with a slope of m = 2 (violet lines), given as a result of the alteration of plagioclase (An- and Ab-components). Thus, the fluids will develop along these lines, parallel to the metastable extension of the albite (resp. analcime) – stilbite phase boundary. The location of the trend-line in the phase diagram is given by X_{An}, the An/(An+Ab) ratio, and SI_{Qz}. The monzonite-waters follow generally a trend-line with higher X_{An} and the Bt-Ms-waters a trend-line with significantly lower X_{An}. The different X_{An} in the fluids are given by the different X_{An} in the rock samples. However, due

to the higher solubility of anorthite than albite (Lasaga et al., 1994) lower X_{An} in the solid phase are expected compared to the fluid phase (Orville, 1972),

5.2 Alteration experiments and reaction processes

Similar activity diagrams were prepared for the alteration experiments at 200°C. The Na-K stability diagram (Fig. 8) shows the dependency of the Na- and K-activity on pH (expressed as H^+) at 200°C and for different saturation states with respect to quartz (SI_{Qz} = 0.0, SI_{Qz} = -0.3, SI_{Qz} = -0.4), since saturation as well as undersaturation was calculated using the code PHREEQE (Parkhurst et al. 1980). Generally, saturation with respect to quartz was significantly lower in the alteration experiments with monzonite compared to the experiments with granite. In the granite experiments some fluids even showed saturation with respect to quartz.

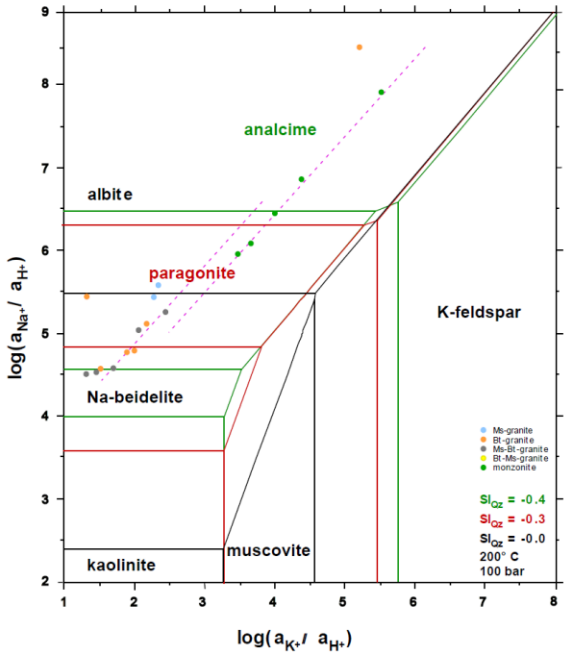

Figure 8: Stability diagram of K vs. Na activity of the waters from the alteration experiments in dependence of pH for 200°C, 100 bar pressure and different quartz saturation states, calculated with the thermodynamic program MacIIPtax (Brown et al., 1989) on the basis of thermodynamic data of Helgeson et al. (1981), Berman (1988), Liou et al. (1991) and phase plotter of Lieberman (1991). Red and green labeling: quartz undersaturation.

Fig. 8 shows that the phase boundary between kaolinite and muscovite is independent of SI_{Qz} (eq. 6), in contrast to the phase boundary between kaolinite and Na-beidellite, shifting in vertical direction with decreasing SI_{Qz} (eq. 5). With increasing undersaturation with respect to quartz a new stability field initially for paragonite and thereafter additionally for analcime develops. The fluids plot in dependence of SI_{Qz} into the Na-beidelite-, paragonite-, and analcime-, resp. albite-, window and can be fitted to varying continuous lines with a slope of m = 1 (violet lines). Thus, the fluids will develop along this line, a parallel to the metastable extension of the albite (resp. analcime) – K-feldspar phase boundary. They will then evolve along this vertical phase boundary until saturation with respect to albite, resp. analcime, is reached, depending on the saturation state with respect to quartz. Thus, the fluids of the two alteration experiments with the lowest SI_{Qz} and which are plotting in the upper part of the presented analcime-window (Fig. 8), showed analcime on the altered rock surface. The potassium concentration in the fluids of the alteration experiments with monzonite is significantly higher than in the fluids of the experiments with granite (Fig. 4). Thus, the data of the alteration experiments with monzonite follow in Fig. 8 a continuous line to the right of the granite data. Fig. 8 shows that the monzonites are like in the leaching experiments the most reactive rocks. Therefore, the monzonite-fluids are the most evolved fluids. Whereas the alteration experiments with granite in most cases show significantly lower reactions.

6. CONCLUSION

The composition of the leachates, simulating a window in the descending path of infiltrating meteoric water (Fig. 1), is clearly related to the composition and nature of the minerals present in the rocks. The amount of water extractable solutes is very different for granites and monzonites, which reflects the petrographic and mineral compositional differences between the two rock types. The origin of the solutes is related to alteration of K-feldspar (K), of biotite and secondary chlorite (K, Mg), to alteration of plagioclase (Na, Ca) and opened fluid inclusions (Na, Cl). The dominant primary anion is chloride which resides in fluid inclusions, in the crystal lattice of minerals, and along grain boundaries. The typical composition of groundwater in crystalline basement rocks indicates that dissolution of the major components of basement rocks, feldspar and mica, essentially dominates the chemical evolution of the waters (and that the reaction with the granitoid rock matrix is the major source of cations). Both mass balance and partial chemical equilibrium control the composition of groundwater in crystalline rock aquifers. With the aid of phase-diagrams the evolution path of these waters are shown.

According to the alteration experiments, simulating the deepest part of the circulating path (Fig. 1), fluid-rock-interaction provoked major textural and chemical alteration of the granitoids mainly by dissolution-precipitation processes. Main effects in the solid rock are: (1) dissolution of quartz, K-feldspar, and plagioclase, (2) alteration of K-feldspar to albite and of biotite to chlorite and hematite, (3) precipitation of illite and subsequently of analcime on the K-feldspar surfaces.

All deep crystalline waters are rich in chloride. Possible original sources of chlorine include minerals like biotite and amphibole, often containing chloride. Salty fluid inclusions are present in all crystalline rocks, mainly in quartz, thus during alteration processes saline fluid could be discharged (Peters 1986, Bucher & Stober 2002). However, a fresh fracture does not intersect many fluid inclusions in quartz compared with the freshly exposed reactive feldspar surfaces and the unstable feldspar will be exposed to water for a very long period of time. Thus, feldspar hydrolyses continuously makes its contribution to the water chemistry (Stober & Bucher 1999). Typical deep waters are near neutral, and also with respect to pH. Another characteristic feature of deep waters in the basement is their low carbonate alkalinity. Thus, the high TDS of the deep waters is not a consequence of prolonged acid-base reaction of water with the primary unstable minerals of the basement rocks, but rather the mechanism of zeolite formation from feldspar that generates saline neutral waters. Zeolitisation does not affect pH and chemically binds free H_2O into the structure of a framework

silicate, and thus increasing passively the TDS of the remaining water (Stober & Bucher 2004).

In contrast to the above described very slow descent of the originally meteoric water, ascent of deep thermal water along the permeable damage zone (or fracture zones) is fast (Fig. 1). During upwelling, p/T-conditions change again, thus also the saturation state of the water with respect to minerals in the damage zone of the fault. In consequence, some minerals will precipitate (i.e. barite, calcite) and hence will clog flow-paths, leading to a reduction of permeability. Thus, continuously flowing thermal springs require tectonically active areas (earthquakes), re-activating the flow path, as a continuous process.

ACKNOWLEDGEMENTS

This research is supported by the German Federal Ministry for Economic Affairs and Energy with the projects "Geofaces-SD" (BMWi, no: 0324025C) and by the state Baden-Württemberg with the project "GeoCool" (no: L7517004). We thank Kurt Bucher for discussion.

REFERENCES

Berman, R.G.: Internally-Consistent Thermodynamic Data for Minerals in the System: Na2O- K2O- CaO- MgO- FeO- Fe2O3- Al2O3- SiO2- TiO2- H2O- CO2. Journal of Petrology, 29(2), 445-522. (1988).

Brown, G.H., Berman, R.G., Perkins, E.H.: PTA-SYSTEM; a Ge0-Calc software package for the calculation and display of activity-temperature-pressure phase diagrams. American Mineralogist, 74, 485-487. (1989).

Bucher, K., Stober, I.: Water-rock reaction experiments with Black Forest gneiss and granite. In: Stober, I., Bucher, K. (eds.): Water-Rock Interaction. KLUWER academic Publishers, 61-96, Dordrecht, The Netherlands. (2002).

Choi, J.H., Edwards, P., Ko, K., Kim, Y.S.: Definition and classification of fault damage zones: a review and a new methodological approach. Earth Sci. Rev., 152, 70–87. (2016).

Emmermann, R.A.: Petrogenetic model for the origin and evolution of the Hercynian granite series of the Schwarzwald. N. Jb. Miner. Abh., 128, 219-253. (1977).

Frogner, P. & Schweda, P.: Hornblende dissolution kinetics at 25°C. Chemical Geology, 151, 169-179. (1998).

Govindaraju, K.: Compilation of working values and sample description for 383 geostandards. Geostandards and Geoanalytical Research, 18(S1), 1-158, (1994).

Grasby, S.E., Hutcheon, I.: Controls on the distribution of thermal springs in the southern Canadian Cordillera. Can. J. Earth Sci, 38, 427–440. (2001).

Helgeson, H.C., Kirkham, D.H., Flowers, G.C.: Theoretical prediction of the thermodynamic behavior of aqueous electrolytes by high pressures and temperatures; IV, Calculation of activity coefficients, osmotic coefficients, and apparent molal and standard and relative partial molal properties to 600 °C and 5 kb. Am. J. Sci., 281, 1249-1516. (1981).

Lasaga, A.C., Soler, J.M., Ganor, J., Burch, T.E., Nagy, K.L.: Chemical weathering rate laws and global geochemical cycles. *Geochimica et Cosmochimica Acta*, *58*(10), 2361-2386. (1994).

Lieberman, J., Petrakakis, K.: TWEEQU thermobarometry; analysis of uncertainties and applications to granulites from western Alaska and Austria. Can. Min., 29, 857-887. (1991).

Liou, J.G., de Capitani, C., Frey, M.: Zeolite equilibria in the system CaAl2Si2O8-NaAlSi3O8-SiO2-H2O. New Zealand Journal of Geology and Geophysics, 34, 293-301. (1991).

López, D.L., Smith, L.: Fluid flow in fault zones: analysis of the interplay of convective circulation and topographically driven groundwater flow. Water Resources Research, 31, 1489–1503. (1995).

Middlemost, E.A.K.: Naming Materials in the Magma/Igneous Rock System. Earth-Science Reviews, 37, 215- 244. (1994).

Orville, P.M.: Plagioclase cation exchange equilibria with aqueous chloride solution: results at 700 °C and 2000 bars in the presence of quartz. Am. J. Sci., 272, 234–272. (1972).

Parkhurst, D.L.: PHREEQC; a computer program for geochemical calculations. U.S. Geol. Surv. Wat. Resour. Investig. Reports, 80(96), 1-195. (1980).

Pauwels, H., Fouillac, C., Fouillac, A.M.: Chemistry and isotopes of deep geothermal saline fluids in the upper rhine graben - origin of compounds and water-rock interactions. Geochim. Cosmochim. Acta, 57, 2737-2749. (1993).

Peters, T.: Structurally incorporated and water extractable chlorine in the Boettstein granite (N. Switzerland). Contributions to Mineralogy and Petrology, 94, 272–3. (1986).

Stober, I., Bucher, K.: Origin of salinity of deep groundwater in crystalline rocks. Terra Nova, 11, 181-185. (1999).

Stober, I., Bucher, K.: Fluid Sinks within the Earth's Crust. Geofluids, 4, 143-151. (2004).

Stober, I., Bucher, K.: Hydraulic conductivity of fractured upper crust: insights from hydraulic tests in boreholes and fluid- rock interaction in crystalline basement rocks. Geofluids, 15(1-2), 161-178. (2015).

Stober, I., Zhong, J., Zhang, L., Bucher, K.: Deep hydrothermal fluid–rock interaction: the thermal springs of Da Qaidam, China. Geofluids, 16, 711-728. (2016).